

Polymer-Bound Pyrene-4,5,9,10-tetraone for Fast-Charge and -Discharge Lithium-Ion Batteries with High Capacity

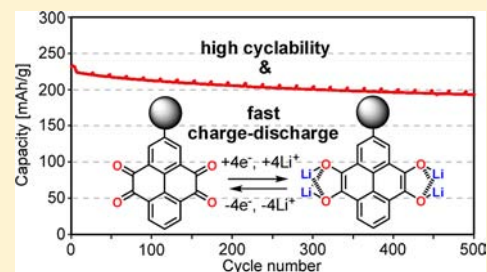
Toshiki Nokami,^{†,§} Takahiro Matsuo,[†] Yuu Inatomi,[‡] Nobuhiko Hojo,[‡] Takafumi Tsukagoshi,[‡] Hiroshi Yoshizawa,[‡] Akihiro Shimizu,[†] Hiroki Kuramoto,[†] Kazutomo Komae,[†] Hiroaki Tsuyama,[†] and Jun-ichi Yoshida^{*,†}

[†]Department of Synthetic Chemistry and Biological Chemistry, Graduate School of Engineering, Kyoto University, Nishikyo-ku, Kyoto City, Kyoto 615-8510, Japan

[‡]R&D Material & Process Development Center, Panasonic Corporation, Nishi-kadoma District, Corporate R&D Division, 1006 Kadoma, Kadoma City, Osaka 571-8501, Japan

S Supporting Information

ABSTRACT: Organic rechargeable batteries have received significant research interest from the viewpoints of structural diversity and sustainability of electrode materials. We designed core structures of organic cathode materials for lithium-ion (Li-ion) batteries based on density functional theory (DFT) calculations, which indicated that six-membered cyclic 1,2-diketones serve as excellent core structures because of the high redox energy change resulting from favorable coordination of the oxygen atoms to Li and the aromaticity of the reduced form. Here, we show that the Li-ion battery composed of pyrene-4,5,9,10-tetraone (PYT), which has two six-membered cyclic 1,2-diketone units, bound to polymethacrylate exhibits remarkable charge–discharge properties with a high specific capacity of 231 mAh/g, excellent rechargeability (83% of the capacity retained after 500 cycles), and charge–discharge ability (90% of the capacity at 30 C as compared to 1 C) in the LiNTf₂/tetraglyme ionic-liquid system.



INTRODUCTION

Rechargeable batteries have already played a major role in power supply for electronic devices, tools, and vehicles.¹ The importance of rechargeable batteries is still increasing because of their potential as storage devices for effective use of renewable energies.² Among various types of rechargeable batteries, Li-ion batteries,³ which are based on the exchange of Li ions between a graphite anode and the layered heavy metal–oxide cathode, are the most popular and powerful rechargeable batteries. However, new cathode materials for rechargeable batteries with high power and capacity that do not contain heavy metals are highly desired from a viewpoint of sustainability.

Organic materials for batteries have received much attention because of their beneficial properties such as being lightweight, flexibility,⁴ and availability from easily accessible natural sources.⁵ Both organic anode⁶ and cathode materials have received significant research interest. Especially, various organic cathode materials such as polyacetylenes,⁷ organosulfur compounds,⁸ *para*-quinones,⁹ other carbonyl compounds,¹⁰ trioxotriangulene,¹¹ tetracyano quinodimethane (TCNQ),¹² bipolar porous polymeric frameworks,¹³ and the composite of polypyrrole with lignin¹⁴ have been studied for several decades. Organic radical polymers have already developed as battery materials, which show a significant battery performance from the viewpoint of power density.¹⁵ Moreover, these organic redox-active polymers are useful not only cathode materials but

also anode materials for an all-organic radical battery and polymer/air batteries.¹⁶ Although extensive studies have been made, there is still a great demand for organic materials that allow for fast charging and discharging with high cyclability for the storage of electrical energy in practical use.

We initiated our project on organic cathode materials for Li-ion batteries based on our experience in organic electrochemistry¹⁷ and organolithium chemistry.¹⁸ Versatility of chemical structures is a benefit of functional materials based on organic molecules. Although there are various types of redox-active functional groups, it is preferable to choose those consisting of atoms in the second row of the periodic table because of their low atomic weights, availability, and sustainability. Thus, we focus on molecules that consist of hydrogen, carbon, nitrogen, and oxygen, and we found that the polymer (polymethacrylate) bearing pyrene-4,5,9,10-tetraone (PYT)¹⁹ as a redox-active core exhibited remarkable charge–discharge properties as a cathode material in a Li-ion battery. In this Article, we report the results of this study.

EXPERIMENTAL SECTION

Materials, methods, preparation, and characterization of 2-amino-pyrene-4,5,9,10-tetraone (PYT-NH₂), NMR spectra, IR spectra, thermal analysis, an additional SEM image and nitrogen-atom mapping

Received: July 18, 2012

Published: November 7, 2012

of the cross section, and cyclic voltammetry plots at several scan rates are provided in the Supporting Information.

Synthesis of Polymer-Bound Pyrene-4,5,9,10-tetraone (PPYT). PYT-NH₂ was prepared from PYT in 61% yield (two steps) (Supporting Information, pp S10,S11). PYT-NH₂ (0.5 mmol, 139 mg) was added to a mixture of (4-dimethylaminopyridine) DMAP (0.07 mmol, 8 mg), poly(methacryloyl chloride) (PMAC) (105 mg), and dry pyridine (5 mL), and the mixture was heated at 60 °C with stirring for 12 h. Next, dry methanol (0.5 mmol) was added and stirred for an additional 10 h at 60 °C. The reaction mixture was cooled to room temperature and poured into methanol (200 mL). The thus-obtained purple precipitate was filtered and dissolved into DMF (4 mL). The DMF solution of polymer was poured into methanol (100 mL). The resulting brown precipitate was filtered and dried under vacuum. Washing with CH₂Cl₂ and drying under vacuum afforded the PPYT as an orange powder (170 mg). Chemical shifts are reported using methylene signals of DMSO at δ 2.50 as an internal standard. Selected signals for PPYT are given. ¹H NMR (600 MHz, DMSO-*d*₆, at 50 °C): δ 0.5–2.8 (alkylH), 6.6–9.0 (aromaticH). ¹³C NMR (solid state, 400 MHz, at 25 °C): δ 16–60 (aliphatic C), 122–143 (aromatic C), 170–182 (carbonyl C). IR (neat): 1184, 1273, 1339, 1431, 1682 cm⁻¹.

Preparation of Electrodes and Battery Cells. Cathodes were prepared by mixing PPYT with acetylene black (AB; Denki Kagaku Kogyo) and poly(vinylidene fluoride) (PVDF; Kureha Chemical Co.) as a binder (ratio: 1.5/4.0/1.0 wt %). These materials were mixed with (*N*-methyl-2-pyrrolidone) NMP as a solvent, and the thus-obtained paste was coated on aluminum sheet using a coater. Next, NMP was removed under vacuum at 85 °C for 1 h.

Hermetically sealed two-electrode cells were used for electrochemical experiments. The cathode (weight ca. 7.0 mg; diameter 12.5 mm) was separated from the lithium anode (The Honjo Chemical Corp.) by the polyethylene porous film (celgard) imbibed with an equimolar LiNTf₂/G4 salt. The three layers were pressed between two current collectors, one in contact with the cathodic material and the other in contact with a lithium disk.

Electrochemical Analyses. Cyclic voltammetry and galvanostatic experiments were performed using BAS 700D and Solartron 1287. The electrode rate capability was examined at the 1 C rate charge for the discharge ability test (1–30 C) and at the 1 C rate discharge for the charge ability test (1–30 C). All experiments were performed at 45 °C. The charge–discharge capacities were determined on the basis of the weight of PYT or PPYT in the cathode.

Materials Characterization. Cross-section samples were prepared using a JEOL SM-09010 cross-section polisher. SEM measurements of cross-section samples were performed on HITACHI SU-70. Nitrogen-atom mapping was carried out using ULVAC-PHI, Inc. model 670.

Quantitative Analysis of Lithium. After the charge or discharge process, the cathode taken from the battery was washed with ethylmethylcarbonate (EMC) two times and dried under vacuum. The cathode was dissolved in aqueous hydrochloric acid, and the resulting solution was used for quantitative analysis of lithium performed on a Thermo Fisher Scientific iCAP6300 inductively coupled plasma (ICP) spectrometer.

RESULTS AND DISCUSSION

We initiated our project by designing a core structure of organic cathode materials. The simplicity of the core structure is essential from the viewpoints of capacity, availability, and sustainability of the materials. The simplest and most abundant functional group in nature that can be reduced without bond breaking seems to be a carbonyl group. One-electron reduction of a carbonyl group leads to the formation of a radical anion, which contains a negative charge mainly on the oxygen atom (Figure 1a). However, the radical anion is not stable because of an unpaired electron, which is mainly located on the carbon. The coupling of two carbons bearing an unpaired electron leads

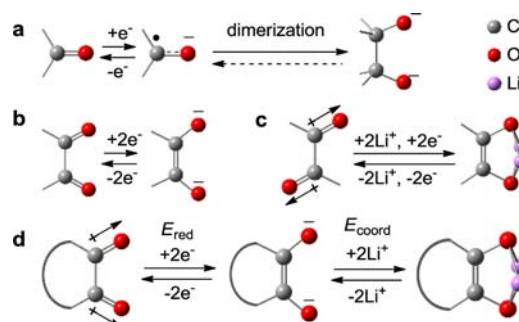


Figure 1. Redox of carbonyl compounds. (a) Redox of a simple carbonyl compound. (b) Redox of 1,2-diketone. (c) Redox of an acyclic 1,2-diketone with lithium ions. (d) Redox of a cyclic 1,2-diketone with lithium ions.

to the formation of a dimer, and such dimerization diminishes the reversibility of the redox processes.

The most straightforward solution to this problem is combining two carbonyl groups at carbons by a covalent bond to make a 1,2-diketone. Two-electron reduction of a 1,2-diketone (one-electron/carbonyl group) leads to the formation of two negatively charged oxygen atoms apart from each other and the formation of one carbon–carbon double bond (Figure 1b). Another important point to be considered is that two oxygen atoms in a 1,2-dicarbonyl compound are suitably located for coordination to Li ions, which are incorporated into the cathode during the course of reduction.

Cyclic 1,2-diketones seem to be superior to acyclic 1,2-diketones, because two carbonyl groups in an acyclic compound tend to direct the opposite way to minimize the repulsion of two dipoles, causing a large structural change (bond rotation) for coordination to Li ions (Figure 1c). Another important point is that repulsion of two dipoles in a cyclic 1,2-dicarbonyl compound, which direct in similar directions, destabilizes the oxidized form, which eventually leads to a higher potential for the battery (Figure 1d).

Next, we examined the effect of the ring size of cyclic 1,2-diketones. We chose benzocyclobutenedione (BBD), acenaphthenequinone (ANQ), and pyrene-4,5-dione (PYD) for representatives of four-, five-, and six-membered ring 1,2-diketones, respectively (Figure 2). The extra π -bonds are

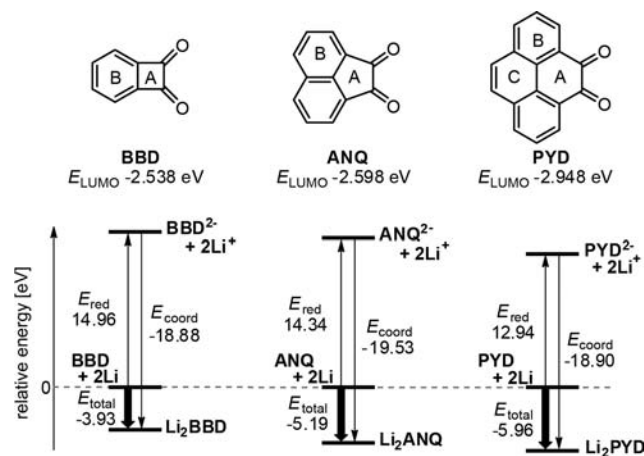


Figure 2. Redox properties of cyclic 1,2-diketones obtained by DFT calculations (B3LYP/6-31G(d)). Relative energies (eV) of the reduced forms without and with Li coordination based on the neutral form.

introduced in the ring using fused benzene structures to ensure the planarity of the cyclic system. Such structures may also enhance chemical stability under redox conditions and increase recyclability of batteries. The redox properties of BBD, ANQ, and PYD were estimated using density functional theory (DFT) calculations (Figure 2 and Supporting Information, Tables S1–S9, S13).²⁰ The lowest-unoccupied molecular orbital (LUMO) energy level of the six-membered ring compound PYD (−2.948 eV) is lower than those of the four- and five-membered ring compounds (BBD and ANQ, −2.538 and −2.598 eV, respectively), indicating favorable one-electron reduction of PYD as compared to BBD and ANQ. The calculated energy change for two-electron reduction is also sensitive to the ring size. The reduction of PYD ($E_{\text{red}} = 12.94$ eV) is energetically more favorable than those of BBD and ANQ (14.96 and 14.34 eV, respectively). The effect of Li coordination is also sensitive to the ring size, and the five-membered ring ANQ enjoys the largest stabilization by coordination (−19.53 eV). As to the net energy change, the six-membered ring compound PYD is the highest (−5.96 eV for two-electron reduction), leading to the highest voltage of the battery.

To obtain a deeper insight into the ring-size effect, the nucleus-independent chemical shifts (NICS),²¹ which are known to serve as a good index of aromaticity, were calculated (Supporting Information, Table S14). A large positive shift of the NICS(1)²² value for the four-membered-ring (ring A) of BBD indicates significant destabilization of the reduced form by virtue of antiaromaticity.²³ On the other hand, a large negative shift for NICS(1) value for the six-membered ring (ring A) of PYD indicates significant stabilization of the reduced form by virtue of an increase in aromaticity. The NICS(1) values for the five-membered ring (ring A) of ANQ do not change significantly, indicating that there is no appreciable stabilization/destabilization upon reduction. In short, the DFT calculations suggest that six-membered ring 1,2-diketones serve as the best candidates for cathode materials.

Experimental studies on the redox properties of cyclic 1,2-diketones BBD, ANQ, and PYD were carried out using cyclic voltammetry in 0.1 M $\text{Bu}_4\text{NBF}_4/\text{N,N}$ -dimethylformamide (DMF) (Figure 3). The increase in the ring size causes a positive shift in the reduction peak potentials (first reduction peak, BBD −1.64 V, ANQ −1.39 V, PYD −1.11 V vs Fc/Fc^+ ; second reduction peak, BBD −2.55 V, ANQ −2.29 V, PYD −1.97 V vs Fc/Fc^+), and this trend is consistent with the DFT calculations. The use of LiBF_4 as the supporting electrolyte resulted in redox potential shifts to less negative potentials, presumably because of the coordination of the oxygen atoms to Li ions.

On the basis of computational and experimental studies on the redox behavior of cyclic 1,2-diketones, we chose to study pyrene-4,5,9,10-tetraone (PYT), which contains two six-membered-ring 1,2-diketone units as a core structure for the cathode material (Figure 4). PYT is expected to undergo four-electron reduction, and the theoretical capacity is 408 mAh/g. The redox energy change obtained by DFT calculations is −11.98 eV, indicating a mean voltage of 3.00 V (Supporting Information, Tables S10–S13).

In general, the use of a low-molecular-weight organic molecule as a cathode material in a Li-ion battery leads to undesired dissolution of the material in the organic solvent during the course of charge–discharge processes. Indeed, the capacity of the PYT/Li battery, which contained PYT as a

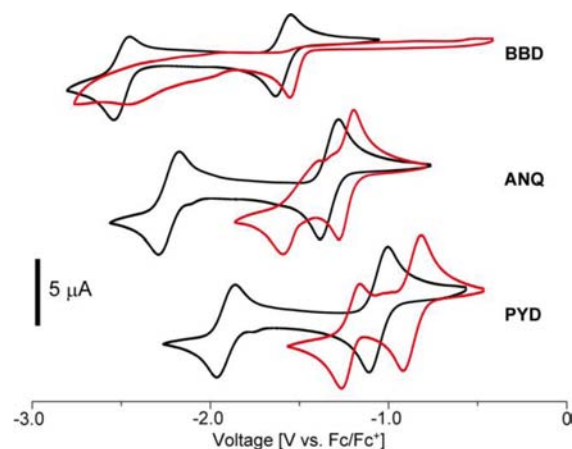


Figure 3. Cyclic voltammograms of cyclic 1,2-diketones BBD, ANQ, and PYD. Black lines: in 0.1 M $\text{Bu}_4\text{NBF}_4/\text{DMF}$ (1.0 mM; working electrode (WE), glassy carbon (GC); counter electrode (CE), platinum plate; reference electrode (RE), Ag/AgNO_3). Red line: in 0.1 M LiBF_4/DMF (1.0 mM; WE, GC; CE, platinum plate; RE, Ag/AgNO_3). Potentials were corrected using ferrocene (Fc/Fc^+) as an internal standard.

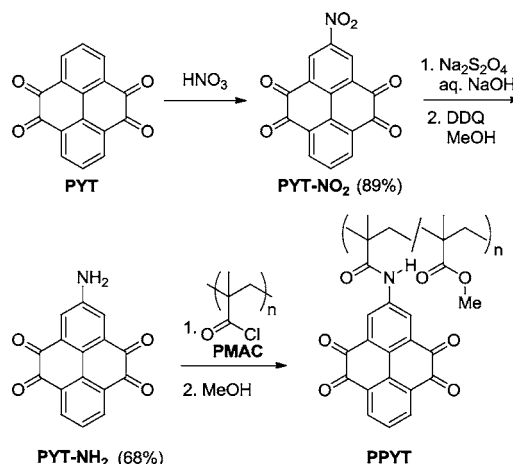


Figure 4. Synthesis of PPYT.

cathode material, significantly decreased during the charge–discharge cycling (Supporting Information, Figure S1). To avoid such a problem, polymer-bound pyrene-4,5,9,10-tetraone (PPYT) was synthesized. After many trials, we chose to use polymethacrylate as a polymer support in anticipation of its physical flexibility and affinity to Li ions, because Li-ion transport inside the polymer structure is crucial for charge–discharge processes. The synthesis is simple and straightforward. Nitration of PYT using HNO_3 gave 2-nitropyrene-4,5,9,10-tetraone (PYT- NO_2). Reduction of PYT- NO_2 with $\text{Na}_2\text{S}_2\text{O}_4$ followed by treatment with 2,3-dichloro-5,6-dicyano-*p*-benzoquinone (DDQ) gave 2-aminopyrene-4,5,9,10-tetraone (PYT- NH_2). The reaction of PYT- NH_2 with PMAC (molecular weight was determined after treatment with MeOH; $M_n = 4600$, $M_w = 10\,600$, polydispersity index (PDI) = 2.29, determined by gel-permeation chromatography (GPC) using poly(methyl methacrylate) (PMMA) as a standard) in the presence of a catalytic amount DMAP in pyridine followed by treatment with methanol gave the target polymer PPYT, in which pyrene-4,5,9,10-tetraone (PYT) units were bound to the polymer backbone by the amide linkage ($M_n = 39\,500$, $M_w =$

56 300, PDI = 1.42, determined by GPC using a polystyrene standard, Supporting Information, Figure S4). The unchanged acyl chlorides ($-\text{CO}-\text{Cl}$) of PMAC were converted to methyl ester groups by the treatment with methanol. PPYT was also characterized by ^1H NMR, solid-state ^{13}C NMR, and IR spectroscopies. Melting point and thermal analyses revealed high thermal stability of PYT- NO_2 , PYT- NH_2 , and PPYT, which have PYT as a common structure (Figure 5a–d). All

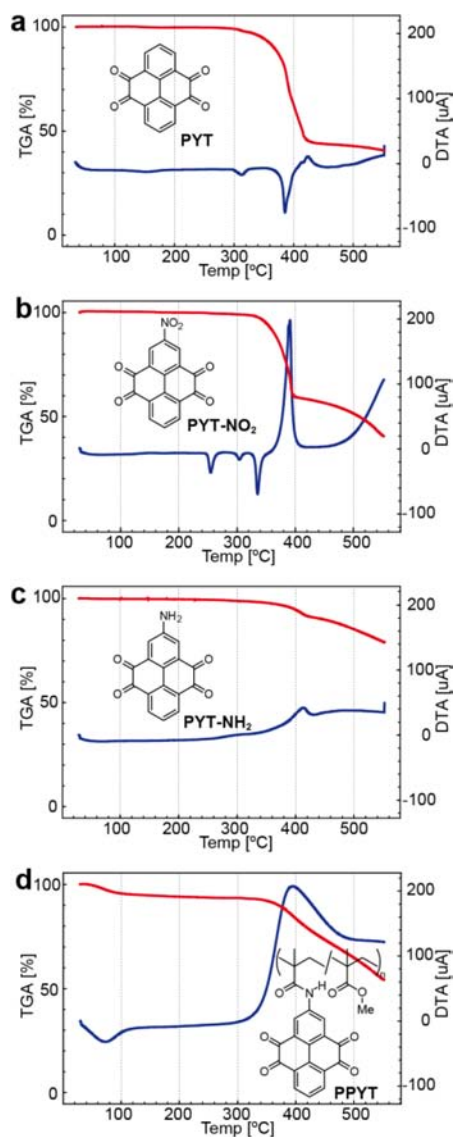


Figure 5. TG-DTA curves of PYT derivatives and PPYT (red lines, TGA [%]; blue lines, DTA [μA]; under nitrogen flow, temperature range 30–550 $^{\circ}\text{C}$, rate 10 $^{\circ}\text{C}/\text{min}$). (a) PYT. (b) PYT- NO_2 . (c) PYT- NH_2 . (d) PPYT.

materials have reasonable thermal stability at around 300 $^{\circ}\text{C}$, which is an important property from a viewpoint of safety of Li-ion batteries. The elemental analysis (N: 3.41 wt %) of PPYT indicated that 1.00 g of the polymer contains 2.44 mmol of PYT units. The theoretical capacity of PPYT is 262 mAh/g.

The cathode was prepared by impregnation of an NMP solution of PPYT into a mixture of AB and PVDF followed by removal of NMP under reduced pressure. The charge–discharge behavior was studied using a coin-type cell equipped with the cathode separated from the lithium anode by a

polyethylene porous film. Cells were imbibed with $\text{LiPF}_6/\text{propylene carbonate}$ (LiPF_6/PC) or an equimolar complex $\text{LiN}(\text{SO}_2\text{CF}_3)_2/\text{tetraglyme}$ ($\text{LiNTf}_2/\text{G4}$), which behaves as a room-temperature ionic liquid.²⁴ The scanning electron microscopy (SEM) images shown in Figure 6a–d indicate

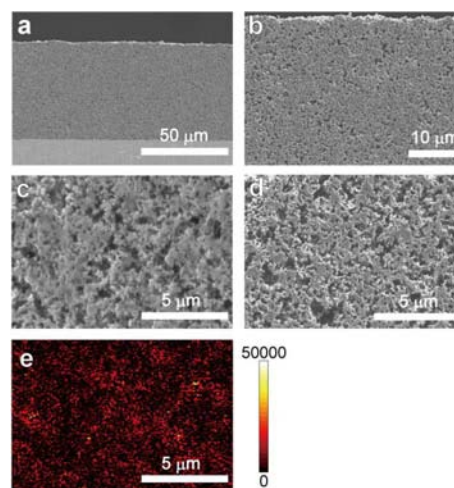


Figure 6. SEM images and N-mapping of the cross section of the charged and discharged cathodes of PPYT/Li battery. (a) Charged (magnification $\times 1000$). (b) Charged ($\times 3000$). (c) Charged ($\times 10000$). (d) Discharged ($\times 10000$). (e) Nitrogen-atom mapping of the charged cathode was obtained by auger electron spectroscopy (AES) at 10 kV. Pixels were colored according to gradient ranges from yellow (high intensity) to red (medium intensity) to black (low intensity) based on the relative intensity of the peak at 382 eV derived from nitrogen atom.

the porous structures of the charged and discharged cathodes, which may facilitate the ion transport in the cathode. The mapping of nitrogen atom was also performed to confirm the uniform distribution of PPYT in the cathode (Figure 6e).

The cyclic voltammograms of the electrodes containing PYT and PPYT are shown in Figure 7. Their overall redox behaviors are similar, indicating that the polymer backbone does not appreciably affect the redox behavior (Figure 7a). The peak current for PPYT increased linearly with an increase in the sweep rate, indicating that mass transfer is not rate-determining (Figure 7b).

The battery exhibited reversible two-stage discharge–charge behavior with average discharge voltage of ca. 2.8 and 2.2 V vs Li/Li^+ (Figure 8), consistent with two major redox waves observed in cyclic voltammetry. The initial discharge capacity was 231 mAh/g (88% of the theoretical value of PPYT based on four-electron transfer), indicating that four-electron reduction took place. Therefore, two major redox waves (ca. 2.8 and 2.2 V) observed in CV seem to correspond to two two-electron redox processes. Theoretical calculations also indicate two two-electron redox processes. The first two redox energies (–3.71 and –3.57 eV) are very close (Supporting Information, Table S15). The second two redox energies (–2.38 and –2.31 eV) are also very close. In fact, each wave of PPYT seems to consist of two redox waves. Careful observation indicates that the first wave has two peaks (3.0 and 2.8 V vs Li/Li^+) and that the second wave also seems to consist of two waves (Figure 7b). To gain further insight into the charge–discharge mechanism, the content of Li in the cathode (containing 0.821 mg of PPYT) was determined by elemental analysis. The

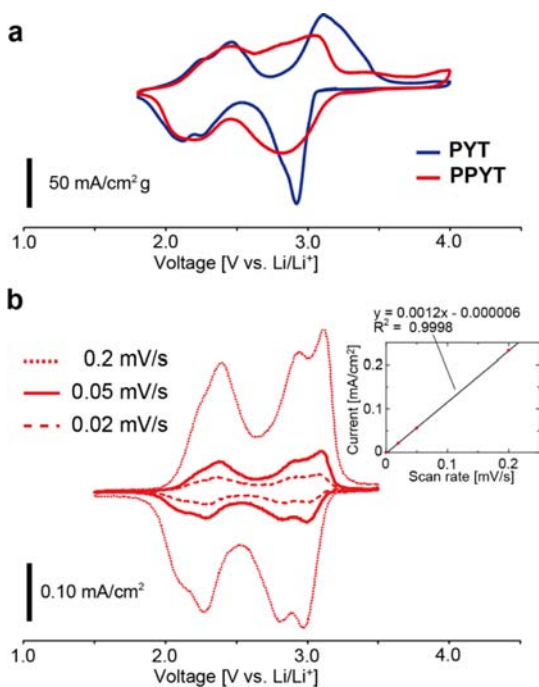


Figure 7. (a) Cyclic voltammograms of an electrode containing PYT and PPYT in 1 M LiPF₆/PC at 45 °C. Scan rate: 0.05 mV/s. Normalized current (mA/cm² g) per gram of redox-active material. (b) Cyclic voltammograms of an electrode containing PPYT in LiNTf₂/G4 at 45 °C and current–scan rate relation at 3.0 V vs Li/Li⁺. Scan rate: 0.2, 0.05, 0.02 mV/s.

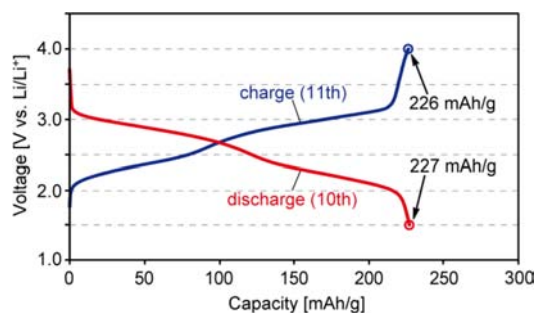


Figure 8. Charge–discharge curves (0.2 C rate) in LiNTf₂/G4 at 45 °C.

cathode contained 0.062 mg of Li after the 10th discharge process, while it contained 0.0069 mg of Li after the 11th charge process. The amount of removed Li (0.0550 mg; 259 mAh/g) is consistent with the mechanism involving reversible insertion of Li into the cathode,²⁵ although a small amount of Li remained in the cathode after the charging process.

To our surprise, the present battery system exhibited fast charge–discharge ability. The cell was successively discharged (Figure 9a) or charged (Figure 9b) at increasing rates (1 C, 3 C, 5 C, 10 C, 20 C, and 30 C). A rate of n C corresponds to a full discharge in $1/n$ h. Even at 30 C, which corresponds to a time of 2 min to fully discharge, the capacity was about 90% of that at the 1 C rate, implying that the present battery is suitable for high-power applications. The physical flexibility and affinity to Li ions of methacrylate polymer backbone seem to be responsible for fast charge–discharge ability, although the details are not clear at present.

High rechargeability of the present battery system is also worth noting (Figure 10). Even after 500 charge–discharge

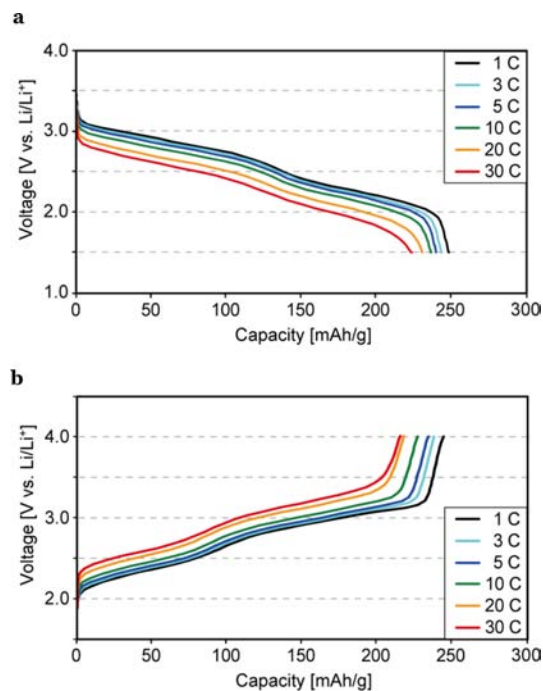


Figure 9. Charge–discharge curves at various rates. (a) Discharge rate capability (1–30 C) in LiNTf₂/G4 at 45 °C. (b) Charge rate capability (1–30 C) in LiNTf₂/G4 at 45 °C.

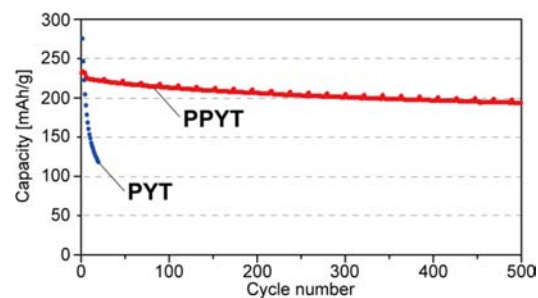


Figure 10. Extended charge–discharge cycling of PPYT and PYT in LiNTf₂/G4 at 45 °C. PPYT (red dots, 500 cycles, 1 C rate), PYT (blue dots, 20 cycles, 0.2 C rate).

cycles at the rate of 1 C (0.2 C every 20 times), 83% (first cycle, 231 mAh/g; 500th cycle, 193 mAh/g) of the capacity of the material was retained. The average Coulombic efficiency between the first and the 500th cycle is 99.96%, which is significantly higher than that of PYT (95.21% between the first and 20th cycle).

CONCLUSIONS

Density functional theory (DFT) calculations and cyclic voltammetric studies indicated that six-membered cyclic 1,2-diketones serve as excellent core structures for cathode materials because of the high redox energy change resulting from favorable coordination of the oxygen atoms to Li and the aromaticity of the reduced form. Pyrene-4,5,9,10-tetraone (PYT), which contains two six-membered-ring 1,2-diketone units, was chosen as a redox core structure because of its favorable capacity, and poly(methacrylate) bearing PYT was synthesized. The cyclic voltammetric studies using the cathode prepared from PPYT, which has the porous structure, indicated that mass transfer is not rate-determining. The battery using

PPYT exhibited excellent charge–discharge ability based on a reversible Li insertion mechanism. High-capacity, fast charge–discharge ability, and excellent cyclability speak well for the high potential of organic materials for Li-ion batteries, and open a new aspect of energy storage. Further work is in progress to explore the detailed mechanism and to develop practical batteries for high-capacity high-power applications.

■ ASSOCIATED CONTENT

● Supporting Information

Additional information as noted in the text. This material is available free of charge via the Internet at <http://pubs.acs.org>.

■ AUTHOR INFORMATION

Corresponding Author

yoshida@sbchem.kyoto-u.ac.jp

Present Address

[§]Tottori University, Graduate School of Engineering, Department of Chemistry and Biotechnology

Notes

The authors declare no competing financial interest.

■ ACKNOWLEDGMENTS

We thank Professor Benoît Champagne in Facultés Universitaires Notre-Dame de la Paix (FUNDP), Belgium, for the use of computers and the program for the theoretical calculations, and Professor Susumu Kitagawa and Dr. Munehiro Inukai for solid-state NMR measurements.

■ REFERENCES

- (1) Armand, M.; Tarascon, J.-M. *Nature* **2008**, *451*, 652–657.
- (2) (a) Lindley, D. *Nature* **2010**, *463*, 18–20. (b) Tarascon, J.-M. *ChemSusChem* **2008**, *1*, 777–779.
- (3) (a) Bruce, P. G.; Freunberger, S. A.; Hardwick, L. J.; Tarascon, J.-M. *Nat. Mater.* **2012**, *11*, 19–29. (b) Bruce, P. G.; Scrosati, B.; Tarascon, J.-M. *Angew. Chem., Int. Ed.* **2008**, *47*, 2930–2946. (c) Abruña, H. D.; Matsumoto, F.; Cohen, J. L.; Jin, J.; Roychowdhury, C.; Prochaska, M.; van Dover, R. B.; DiSlavo, F. J.; Kiya, Y.; Henderson, J. C.; Hutchison, G. R. *Bull. Chem. Soc. Jpn.* **2007**, *80*, 1843–1855. (d) Whittingham, M. S. *Chem. Rev.* **2004**, *104*, 4271–4301. (e) Tarascon, J.-M.; Armand, M. *Nature* **2001**, *414*, 359–367.
- (4) Nishide, H.; Oyaizu, K. *Science* **2008**, *319*, 737–738.
- (5) Chen, H.; Armand, M.; Demailly, G.; Dolhem, F.; Poizot, P.; Tarascon, J.-M. *ChemSusChem* **2008**, *1*, 348–355.
- (6) (a) Yang, S.; Feng, X.; Müllen, K. *Adv. Mater.* **2011**, *23*, 3575–3579. (b) Yang, S.; Feng, X.; Ivanovici, S.; Müllen, K. *Angew. Chem., Int. Ed.* **2010**, *49*, 8408–8411. (c) Liang, Y.; Schwab, M. G.; Zhi, L.; Mugnaioli, E.; Kolb, U.; Feng, X.; Müllen, K. *J. Am. Chem. Soc.* **2010**, *132*, 15030–15037. (d) Yang, S.; Feng, X.; Zhi, L.; Cao, Q.; Maier, J.; Müllen, K. *Adv. Mater.* **2010**, *22*, 838–842. (e) Yang, S.; Cui, G.; Pang, S.; Cao, Q.; Kolb, U.; Feng, X.; Maier, J.; Müllen, K. *ChemSusChem* **2010**, *3*, 236–239.
- (7) (a) Novák, P.; Müller, K.; Santhanam, K. S. V.; Haas, O. *Chem. Rev.* **1997**, *97*, 207–281. (b) Nigrey, P. J.; MacInnes, D., Jr.; Nairns, D. P.; MacDiarmid, A. G.; Heeger, A. J. *J. Electrochem. Soc.* **1981**, *128*, 1651–1654. (c) MacInnes, D., Jr.; Druy, M. A.; Nigrey, P. J.; Nairns, D. P.; MacDiarmid, A. G.; Heeger, A. J. *J. Chem. Soc., Chem. Commun.* **1981**, 317–319.
- (8) (a) Tomoo, S.; Oyama, N. *J. Electrochem. Soc.* **2010**, *157*, F23–F29. (b) Zhan, L. Z.; Song, Z. P.; Zhang, J. Y.; Tang, J.; Zhan, H.; Zhou, Y. H.; Zhan, C. M. *J. Appl. Electrochem.* **2008**, *38*, 1691–1694. (c) Kiya, A.; Hutchison, G. R.; Henderson, J. C.; Sarukawa, T.; Hatozaki, O.; Oyama, N.; Abruña, H. D. *Langmuir* **2006**, *22*, 10554–10563. (d) Inamasu, T.; Yoshitoku, D.; Sumi-otorii, Y.; Tani, H.; Ono, N. *J. Electrochem. Soc.* **2003**, *150*, A128–A132. (e) Pope, J. M.; Sato,

T.; Shoji, E.; Oyama, N.; White, K. C.; Buttry, D. A. *J. Electrochem. Soc.* **2002**, *149*, A939–A952. (f) Oyama, N.; Tatsuma, T.; Sato, T.; Sotomura, T. *Nature* **1995**, *373*, 598–600. (g) Visco, S. J.; Mailhe, C. C.; De Jonghe, L. C.; Armand, M. B. *J. Electrochem. Soc.* **1989**, *136*, 661–664.

(9) (a) Song, Z.; Xu, T.; Gordin, M. L.; Jiang, Y.-B.; Bae, I.-T.; Xiao, Q.; Zhan, H.; Liu, J.; Wang, D. *Nano Lett.* **2012**, *12*, 2205–2211. (b) Xu, W.; Read, A.; Koech, P. K.; Hu, D.; Wang, C.; Xiao, J.; Padmaperuma, A. B.; Graff, G. L.; Liu, J.; Zhang, J. G. *J. Mater. Chem.* **2012**, *22*, 4032–4039. (c) Yao, M.; Senoh, H.; Sakai, T.; Kiyobayashi, T. *Int. J. Electrochem. Sci.* **2011**, *6*, 2905–2911. (d) Liu, K.; Zheng, J.; Zhong, G.; Yang, Y. *J. Mater. Chem.* **2011**, *21*, 4125–4131. (e) Kassam, A.; Burnell, D. J.; Dahn, J. R. *Electrochem. Solid-State Lett.* **2011**, *14*, A22–A23. (f) Yao, M.; Senoh, H.; Yamazaki, S.; Siroma, Z.; Sakai, T.; Yasuda, K. *J. Power Sources* **2010**, *195*, 8336–8340. (g) Genorio, B.; Pirnat, K.; Cerc-Korosec, R.; Dominko, R.; Gaberscek, M. *Angew. Chem., Int. Ed.* **2010**, *49*, 7222–7224. (h) Oyama, N.; Sarukawa, T.; Mochizuki, Y.; Shimomura, T.; Yamaguchi, S. *J. Power Sources* **2009**, *189*, 230–239. (i) Chen, H.; Armand, M.; Courty, M.; Jiang, M.; Gray, C. P.; Dolhem, F.; Tarascon, J.-M.; Poizot, P. *J. Am. Chem. Soc.* **2009**, *131*, 8984–8988. (j) Armand, M.; Grugeon, S.; Vezin, H.; Laruelle, S.; Ribièrre, P.; Poizot, P.; Tarascon, J.-M. *Nat. Mater.* **2009**, *8*, 120–125. (k) Song, Z.; Zhan, H.; Zhou, Y. *Chem. Commun.* **2009**, 448–450. (l) Tang, J.; Song, Z. P.; Shan, N.; Zhan, L. Z.; Zhang, J. Y.; Zhan, H.; Zhou, Y. H.; Zhan, C. M. *J. Power Sources* **2008**, *185*, 1434–1438. (m) Gall, T. L.; Reiman, K. H.; Gressel, M. C.; Owen, J. R. *J. Power Sources* **2003**, *119–121*, 316–320.

(10) (a) Han, X.; Qing, G.; Sun, J.; Sun, T. *Angew. Chem., Int. Ed.* **2012**, *51*, 5147–5151. (b) Song, Z.; Zhan, H.; Zhou, Y. *Angew. Chem., Int. Ed.* **2010**, *49*, 8444–8448. (c) Walker, W.; Grugeon, S.; Mentre, O.; Laruelle, S.; Tarascon, J.-M.; Wudl, F. *J. Am. Chem. Soc.* **2010**, *132*, 6517–6523. (d) Han, X.; Chang, C.; Yuan, L.; Sun, T.; Sun, J. *Adv. Mater.* **2007**, *19*, 1616–1621.

(11) (a) Morita, Y.; Nishida, S.; Takui, T.; Nakasuji, K. *J. Synth. Org. Chem. Jpn.* **2012**, *70*, 50–59. (b) Morita, Y.; Nishida, S.; Murata, T.; Moriguchi, M.; Ueda, A.; Satoh, M.; Arifuku, K.; Sato, K.; Takui, T. *Nat. Mater.* **2011**, *10*, 947–951.

(12) Hanyu, Y.; Honma, I. *Sci. Rep.* **2012**, *2*, 453.

(13) Sakaushi, K.; Nickerl, G.; Wisse, F. M.; Nishio-Hamane, D.; Hosono, E.; Zhou, H.; Kaskel, S.; Eckert, J. *Angew. Chem., Int. Ed.* **2012**, *51*, 7850–7854.

(14) Milczarek, G.; Inganäs, O. *Science* **2012**, *335*, 1468–1471.

(15) (a) Lin, C.-H.; Chou, W.-J.; Lee, J.-T. *Macromol. Rapid Commun.* **2012**, *33*, 107–113. (b) Dai, Y.; Zhang, Y.; Gao, L.; Xu, G.; Xie, J. *J. Electrochem. Soc.* **2011**, *158*, A291–A295. (c) Suga, T.; Sugita, S.; Ohshiro, H.; Oyaizu, K.; Nishide, H. *Adv. Mater.* **2011**, *23*, 751–754. (d) Nakahara, K.; Oyaizu, K.; Nishide, H. *Chem. Lett.* **2011**, *40*, 222–227. (e) Oyaizu, K.; Kawamoro, T.; Suga, T.; Nishide, H. *Macromolecules* **2010**, *43*, 10382–10389. (f) Nesvadba, P.; Bugnon, L.; Maire, P.; Novák, P. *Chem. Mater.* **2010**, *22*, 783–788. (g) Suguro, M.; Mori, A.; Iwasa, S.; Nakahara, K.; Nakano, K. *Macromol. Chem. Phys.* **2009**, *210*, 1402–1407. (h) Suga, T.; Ohshiro, H.; Sugita, S.; Oyaizu, K.; Nishide, H. *Adv. Mater.* **2009**, *21*, 1627–1630. (i) Nakahara, K.; Iriyama, J.; Iwasa, S.; Suguro, M.; Satoh, M.; Cairns, E. J. *J. Power Sources* **2007**, *165*, 870–873. (j) Nakahara, K.; Iriyama, J.; Iwasa, S.; Suguro, M.; Satoh, M.; Cairns, E. J. *J. Power Sources* **2007**, *163*, 1110–1113. (k) Suga, T.; Pu, Y. J.; Kasatori, S.; Nishide, H. *Macromolecules* **2007**, *40*, 3167–3173. (l) Suga, T.; Konishi, H.; Nishide, H. *Chem. Commun.* **2007**, 1730–1732. (m) Nishide, H.; Suga, T. *Interface* **2005**, *14*, 32–36. (n) Suga, T.; Pu, Y. J.; Oyaizu, K.; Nishide, H. *Bull. Chem. Soc. Jpn.* **2004**, *77*, 2203–2204. (o) Nishide, H.; Iwasa, S.; Pu, Y. J.; Suga, T.; Nakahara, K.; Satoh, M. *Electrochim. Acta* **2004**, *50*, 827–831. (p) Nakahara, K.; Iwasa, S.; Satoh, M.; Morioka, Y.; Iriyama, M.; Suguro, M.; Hasegawa, E. *Chem. Phys. Lett.* **2002**, *359*, 351–354.

(16) Choi, W.; Harada, D.; Oyaizu, K.; Nishide, H. *J. Am. Chem. Soc.* **2011**, *133*, 19839–19843.

(17) (a) Ashikari, Y.; Nokami, T.; Yoshida, J. *J. Am. Chem. Soc.* **2011**, *133*, 11840–11843. (b) Yoshida, J.; Kataoka, K.; Horcajada, R.; Nagaki, A. *Chem. Rev.* **2008**, *108*, 2265–2299. (c) Nokami, T.; Ohata,

K.; Inoue, M.; Tsuyama, H.; Shibuya, A.; Soga, K.; Okajima, M.; Suga, S.; Yoshida, J. *J. Am. Chem. Soc.* **2008**, *130*, 10864–10865. (d) Nokami, T.; Shibuya, A.; Tsuyama, H.; Suga, S.; Bowers, A. A.; Crich, D.; Yoshida, J. *J. Am. Chem. Soc.* **2007**, *129*, 10922–10928. (e) Yoshida, J.; Suga, S. *Chem.-Eur. J.* **2002**, *8*, 2651–2658.

(18) (a) Kim, H.; Nagaki, A.; Yoshida, J. *Nat. Commun.* **2011**, *2*, 264. (b) Tomida, Y.; Nagaki, A.; Yoshida, J. *J. Am. Chem. Soc.* **2011**, *133*, 3744–3747. (c) Nagaki, A.; Miyazaki, A.; Yoshida, J. *Macromolecules* **2010**, *43*, 8424–8429. (d) Nagaki, A.; Tomida, Y.; Miyazaki, A.; Yoshida, J. *Macromolecules* **2009**, *42*, 4384–4387. (e) Nagaki, A.; Kim, H.; Yoshida, J. *Angew. Chem., Int. Ed.* **2008**, *47*, 7833–7836.

(19) Hu, J.; Zhang, D.; Harris, F. W. *J. Org. Chem.* **2005**, *70*, 707–708.

(20) The DFT calculations were performed with the Gaussian 09 program (Supporting Information).

(21) Schleyer, P. v. R.; Maerker, C.; Dransfeld, A.; Jiao, H.; Hommes, N. J. R. v. E. *J. Am. Chem. Soc.* **1996**, *118*, 6317–6318.

(22) Schleyer, P. v. R.; Manoharan, M.; Wang, Z. X.; Kiran, B.; Jiao, H. J.; Puchta, R.; Hommes, N. *Org. Lett.* **2001**, *3*, 2465–2468.

(23) Rieke, R. D.; White, C. K.; Rhyne, L. D.; Gordon, M. S.; McOmie, J. F. W.; Hacker, N. P. *J. Am. Chem. Soc.* **1977**, *99*, 5387–5393.

(24) Yoshida, K.; Nakamura, M.; Kazue, Y.; Tachikawa, N.; Tsuzuki, S.; Seki, S.; Dokko, K.; Watanabe, M. *J. Am. Chem. Soc.* **2011**, *133*, 13121–13129.

(25) Guyomard, D.; Tarascon, J.-M. *Adv. Mater.* **1994**, *6*, 408–412.